Silver−Carbon Cluster AgC_3: Structure and Infrared Frequencies

Yun Wang, Jan Szczepanski, and Martin Vala*

Department of Chemistry and Center for Chemical Physics, University of Florida, Gainesville, Florida 32611-7200

Received: June 12, 2008; Revised Manuscript Received: August 25, 2008

Silver−carbon clusters were formed by dual Nd:YAG laser vaporization, trapped in a solid Ar matrix at 12 K, and investigated by infrared spectroscopy. Two new infrared absorption bands were observed at 1827.8 and 1231.6 cm^{-1}. Isotopic (^{13}C) substitution experiments were performed to aid in their assignment. Possible structures considered for the carrier of these bands were Ag_mC_n with $m = 1$ and 2 and $n = 1-3$, all of which were investigated by density functional theory calculations. The geometries and associated vibrational harmonic-mode frequencies of these clusters were computed with the MPW1PW91 functional and SDD basis set. Both calculations and ^{13}C-isotopic substitution experiments indicate that the new bands are due to the asymmetric and symmetric C═C stretching modes, respectively, in near-linear AgC_3.

1. Introduction

The interaction of metals with carbon has been a topic of long-standing interest. In part, this is the result of the potential involvement of metal−carbon molecules in catalysis.[1,2] Ever since the discovery of the novel metallocarbohedrenes ("met-cars") by Castleman and co-workers,[3] metal−carbon research has accelerated. Met-cars have been formed with the stoichiometry M_8C_{12}, where M = Ti, V, Zr, Nb, Mo, Hf, Cr, or Fe, but they can also be formed with two metals with stoichiometry $Ti_{8-x}M_xC_{12}$, where M = Si, Y, Zr, Nb, Mo, Hf, Ta, or W.[4−7] Other types of clusters have also been studied, including the anionic clusters $V_mC_n^-$ ($m = 1-4$, $n = 2-8$), $Co_2C_n^-$ ($n = 2$, 3), and $Nb_2C_n^-$ ($n = 4-9$), studied by photoelectron spectroscopy and density functional theory (DFT) calculations.[8−10] Wang and co-workers investigated the first-row-transition-metal−C_3 clusters MC_3^- (with M = Sc, V, Cr, Mn, Fe, Co, and Ni), as well as FeC_n^- ($n = 3$, 4), NbC_n^- ($n = 2-7$), and TiC_n^- ($n = 2-5$) also using photoelectron spectroscopy.[11−14] Similar studies on MC_n^- clusters (with M = Sc, Y, La; $n = 5-20$) were reported by Kohno et al.[15] $Cu_nC_2^+$ ($n = 2k + 1$, $k = 1-7$) and $Cu_nC_4^+$ ($n = 2k + 1$, $k = 2-4$) clusters have been studied using time-of-flight mass spectrometry.[16] Cationic CuC_n^+ clusters ($n = 1-3$) were generated in spark discharges of Cu and graphite and observed in mass spectrometric studies.[17] Matrix-isolation vibrational spectroscopy studies of GeC_3Ge, TiC_3, CrC_3, CoC_3, AlC_3, AlC_3Al, and NiC_3Ni were reported by Graham and co-workers.[18−23] Copper and silver polyynides (Cu- and Ag-capped carbynes) have been characterized using Raman spectroscopy.[24] Other properties of metal−carbon clusters including trends in ionization potentials and electronic affinities have been investigated as well.[25,26] Studies of CuC_3 and its photoinduced isotopic scrambling were recently reported by us.[27] Because silver is similar in electron configuration to copper, it is interesting to see whether similar or different silver−carbon clusters are formed.

Only a few reports on silver−carbon clusters have been published. Silver acetylide (AgC≡CAg), one of the oldest organometallics, was synthesized by reacting acetylenic compounds with an ammoniacal silver nitrate solution.[28,29] Cationic AgC_n^+ clusters ($n = 1-3$), generated in a radio-frequency spark ion source, were investigated using mass spectrometric methods.[17]

In this article, we report the first vibrational spectroscopic study of a silver−carbon cluster trapped in solid argon at 12 K. Corresponding theoretical work on small stable silver−carbon clusters, Ag_mC_n ($m = 1$, 2; $n = 1-3$) using density functional calculations has been carried out in the search for the equilibrium geometry and vibrational frequencies of the cluster giving rise to the two new bands observed. Both experiments and calculations indicate that the near-linear AgC_3 cluster is responsible.

2. Experimental Methods

Silver−carbon clusters were generated by two-beam laser ablation of silver and graphite, or in the case of the isotopic studies, a pressed pellet of ^{12}C and ^{13}C (Isotec). The experimental apparatus used for the generation and trapping of silver−carbon clusters in solid argon is similar to that described in a previous article.[27] Briefly, the output of a pulsed Nd:YAG laser (1064/532 nm, 0.2−0.5 W, 10 Hz) was split into two beams, with one beam focused on a small piece of silver sample (SPEX) and the other beam focused on the carbon sample. The reaction products were codeposited with argon gas onto a 12 K CsI window cooled by a closed-cycle helium cryostat (APD Displex). After 2−3 h of deposition, infrared absorption spectra were collected using a Nicolet Magna 560 FT-IR spectrometer (0.5 cm^{-1} resolution). Annealing of the matrix (heating to 35 K and recooling to 12 K), as well as photolysis with a medium-pressure 100-W Hg lamp, were also performed to induce secondary reactions.

3. Computational Methods

All calculations were carried out using the Gaussian 03 suite of programs.[30] The equilibrium geometries, harmonic vibrational frequencies, and dissociation energies were calculated using the MPW1PW91 functional, a modified Perdew−Wang exchange and correlation functional,[31,32] with SDD basis set (the Stuttgart/Dresden ECPs and D95V basis sets for silver and carbon, respectively).[33] In previous work, the SDD basis set was chosen

* To whom correspondence should be addressed. E-mail: mvala@chem.ufl.edu.

10.1021/jp805181m CCC: $40.75
Published on Web 10/10/2008

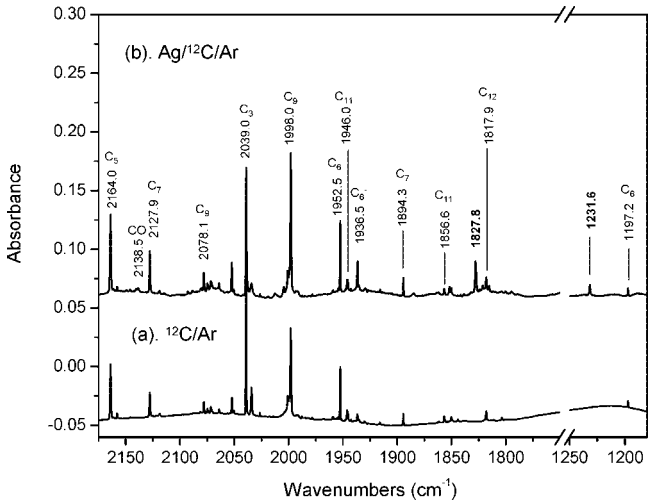

Figure 1. Infrared absorption spectra of products of laser ablation of graphite (spectrum a) and products of two-beam laser ablation of graphite and silver (spectrum b). The spectra were recorded after matrix annealing to 35 K and then cooling back to 12 K. The major bands due to pure carbon clusters and their reaction products with silver at 1827.8 and 1231.6 cm^{-1} are indicated.

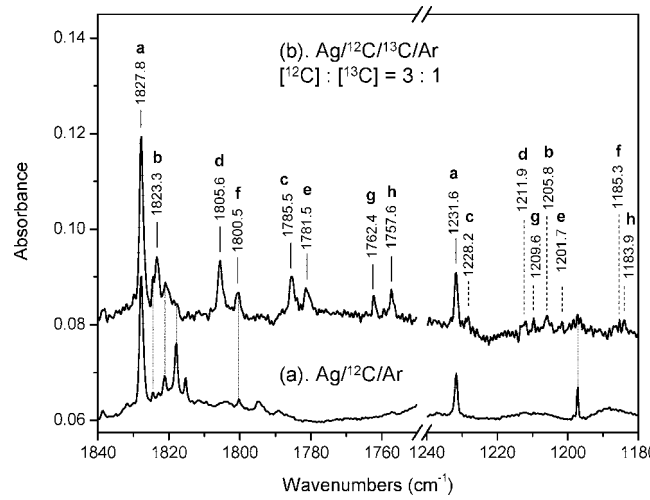

Figure 2. Infrared spectra of reaction products from laser ablation of Ag and ^{12}C (spectrum a) and from laser ablation of Ag and $^{12/13}C$ (spectrum b). The bands marked by vertical dashed lines are tentatively assigned to isotopomeric partners of the 1231.6 cm^{-1} band. The bands marked by vertical dotted lines are due to C_3H (1824.4 cm^{-1}),[45,46] C_2H^+ (1820.2 cm^{-1}),[47] C_{12} (1817.9 cm^{-1}),[48] and C_6 (1197.2 cm^{-1}).[49]

to calculate M—NH_3 (M = Cu, Ag) and M^+—H_2S (M = Cu, Ag, Au) systems.[34,35] The MPW1PW91 functional was recommended by Wiberg,[36] Dunbar,[37] and Oomens et al.[38] for the calculation of C-, H-, and metal-containing systems. The MPW1PW91 functional was also used in our recent studies of iron complexed with cationic and neutral polycyclic aromatic hydrocarbons.[39,40]

In our previous work on the CuC_3 cluster,[27] we compared results calculated by the MPW1PW91 functional and the B3LYP functional (Becke's three-parameter hybrid functional combined with the nonlocal correction functional of Lee, Yang, and Parr).[41] This comparison showed that calculations using the MPW1PW91 functional supported the experimental data, whereas the B3LYP functional did poorly in predicting the ^{13}C-labeled isotopomer frequencies and the relative integral intensities of $^{63}Cu^{12/13}C_3$. Because silver and copper atoms have similar electronic configurations ([Xe]$4d^{10}5s^1$ for Ag and [Ar]$3d^{10}4s^1$ for Cu), we tested the MPW1PW91/SSD level of calculation on the near-linear CuC_3 cluster by comparing the results to those obtained at the MPW1PW91/6-311++(3df) level and to the experimental $^{63}Cu^{12/13}C_3$ isotopomer frequencies.[27] The comparison revealed that the maximum isotopomer frequency differences (after scaling) between MPW1PW91/SSD and experiment is 2.3 cm^{-1}, with an average difference of 1.3 cm^{-1}, compared to the 1.6 and 0.96 cm^{-1}, respectively, for MPW1PW91/6-311++(3df).[27] Although the MPW1PW91/SDD values are slightly higher than the MPW1PW91/6-311++(3df) results, they are still acceptable for isotopic ^{13}C isotopomer frequency matching. For this reason, we used the MPW1PW91/SSD functional/basis set in the present work.

4. Results and Discussion

4.1. Experimental Infrared Spectra. The infrared absorption spectra in the 1180−1250 and 1750−2200 cm^{-1} ranges for the species laser-ablated from graphite and for the species formed by the synchronized dual-laser ablation of silver and graphite are displayed in Figure 1 in panels a and b, respectively. Various neutral carbon clusters (from C_3−C_{12}) were observed in both spectra a and b.[42,43] The band at 1936.5 cm^{-1} in spectrum b was assigned to C_6^-.[44] Impurities such as CO and H_2O are also present, because of the high laser ablation power.[21] A weak band at 1824.4 cm^{-1}, assigned to C_3H,[45,46] was also observed.

Two new bands were observed in spectrum b, at 1827.8 and 1231.6 cm^{-1}. The higher-frequency band is about 3 times more intense than the lower-frequency one. Both were found to be dependent on the silver and carbon concentrations and were thus attributed to a species containing both silver and carbon.

Numerous experiments were performed to determine whether the bands belong to the same species. Different Ag/C ratios were obtained by varying the ablating laser intensities. The two new bands decreased in intensity with lower ablation power and increased with higher power. Matrix annealing to 35 K and recooling to 12 K increased the intensity of both bands by about 25%. UV−visible photolysis with a medium-pressure mercury lamp up to 1 h decreased both bands by about 15%. Under all these different conditions, the integral intensity ratio of the 1827.8 and 1231.6 cm^{-1} bands remained constant (at 3.03 ± 0.3), indicating that they belong to the same species.

Isotopic (^{13}C) substitution is a powerful means of identifying the structures of unknown molecular systems. Figure 2 shows the spectrum of the reaction products of the laser ablation of Ag and ^{12}C (spectrum a) compared to the spectrum of reaction products of laser ablation of Ag and $^{12/13}C$ mixture (spectrum b). There are clearly eight isotopomeric bands (**a**−**h**) built on the 1827.8 cm^{-1} band in the ^{13}C-labeled spectrum. In the lower-energy region (1231.6 cm^{-1} band), eight very weak bands were also observed. They are tentatively assigned here to various isotopomers (see Table 2 below). A similar isotopomer band pattern was previously observed for the near-linear $^{12/13}CuC_3$ cluster,[27] the near-linear $^{12/13}C_3 \cdot H_2O$ complex,[50] and the linear $^{12/13}C_3Cr$ and $^{12/13}C_3Co$ clusters.[20,21] This strongly suggests that the 1827.8 cm^{-1} band should be assigned to the C═C asymmetric stretching mode in linear or near-linear $^{12/13}C_3$ isotopomers bonded at one end to Ag. This preliminary conclusion is supported in the next section by computation of the equilibrium geometries and harmonic frequencies of a number of silver−carbon clusters, including $Ag^{12/13}C_3$.

4.2. Equilibrium Geometries and Vibrations for Ag_mC_n (m=1, 2; n = 1−3) Clusters. A number of metal−carbon clusters of the type MC_3 and MC_3M (M = transition metal) have been studied previously.[18−23,27] Here, we explore theoreti-

TABLE 1: Vibrational Frequencies (cm^{-1}) and Integral Intensities (km/mol) for Electronic Ground States of Ag_mC_n ($m = 1, 2$; $n = 1-3$) Clusters (Displayed in Figure 3), Calculated Using the MPW1PW91/SDD Functional/Basis Sets

Ag_mC_n isomer	MPW1PW91/SDD
A. AgC ($X\ ^4\Sigma$)	σ 477.2 (9)
B. *l*-AgC_2 ($X\ ^2\Sigma$)	σ 2018.5 (34), σ 425.0 (21), π 97.2 (2×2)
C. *c*-AgC_2 ($X\ ^2A_1$)	a_1 1702.2 (16), a_1 369.8 (11), b_2 179.0 (0)
D. *nl*-AgC_3 ($X\ ^2A'$)	a′ 1860.0 (117), a′ 1224.1 (14), a′ 421.9 (35), a′ 335.8 (9), a″ 227.6 (5), a′ 101.4 (17)
E. *c*-Ag_2C ($X\ ^3A_2$)	a_1 388.7 (2), b_2 255.7 (4), a_1 156.1 (0)
F. *l*-Ag_2C ($X\ ^3\Sigma_g$)	σ 417.7 (4), σ 158.7 (1), π 110.7 (1), π 42.5 (0)
G. *l*-Ag_2C_2 ($X\ ^1\Sigma_g$)	σ_g 2092.4 (0), σ_u 600.3 (78), π_g 239.5 (2×0), σ_g 183.9 (0), π_u 83.9 (2×51)
H. *w*-Ag_2C_3 ($X\ ^1A_1$)	b_2 1761.1 (639), a_1 1265.7 (11), a_1 547.3 (0), b_2 449.7 (44), b_1 289.9 (2), a_1 261.5 (9), a_2 215.9 (0), b_2 115.0 (155), a_1 36.4 (4)
I. *c*-Ag_2C_3 ($X\ ^1A_1$)	a_1 1390.4 (721), b_2 1297.4 (0), a_1 355.3 (120), b_2 335.4 (30), b_1 334.2 (4), a_1 317.3 (1), a_1 150.3 (2), b_2 134.8 (10), a_2 120.7 (0)
J. *c*-Ag_2C_3 ($X\ ^1A_1$)	a_1 1705.6 (103), a_1 519.1 (18), b_2 510.0 (0), a_1 465.3 (7), b_2 452.1 (0), a_2 233.3 (0), b_2 187.7 (43), b_1 174.0 (22), a_1 101.3 (0)

cally the AgC, AgC_2, AgC_3, Ag_2C, Ag_2C_2, and Ag_2C_3 clusters. Figure 3 shows the stable equilibrium geometries and relative energies predicted (MPW1PW91/SDD) for these clusters. Harmonic vibrational frequencies and integral intensities are displayed in Table 1.

4.2.1. AgC. The ground-state of diatomic AgC is calculated to be a quartet with a bond length of 2.051 Å. The doublet spin state is higher in energy than the quartet by 0.31 eV. The calculation indicates a very low vibrational integral intensity (9 km/mol), which is probably the reason why AgC was not observed in the experiments.

4.2.2. AgC_2. Two structures, **B** and **C** in Figure 3, are predicted for AgC_2. Linear *l*-AgC_2 (**B**) is marginally more stable by 0.04 eV than cyclic *c*-AgC_2 (**C**). Table 1 shows that the strongest infrared modes in *l*-AgC_2 and *c*-AgC_2 lie at 2018.5 and 1702.2 cm^{-1}, respectively. However, because the calculated integral intensities are relatively low, 34 and 16 km/mol, the absence of these two bands is understandable.

4.2.3. AgC_3. Only one stable structure (**D**) is found for the AgC_3 cluster: the near-linear one, as displayed in Figure 3. The bond lengths and angles calculated at the MPW1PW91/SDD level are marked in the figure. The *nl*-AgC_3 cluster has a doublet spin multiplicity. Searches for doublet bicyclic AgC_3 and cyclic C_3 bonded to Ag resulted in one imaginary frequency for each. Predicted vibrational frequencies (unscaled) and integral intensities for *nl*-AgC_3 are 1860.0 cm^{-1} (117 km/mol) (asymmetric C═C stretch mode) and 1224.1 cm^{-1} (14 km/mol) (symmetric C═C stretch mode). The intensity ratio of the two bands is relatively high (8.36) compared to experiment (3.03 ± 0.3). The B3LYP functional with the SDD basis set was also tested on *nl*-AgC_3. The predicted vibrational frequencies (and integral intensities) are 1864.9 cm^{-1} (133 km/mol) and 1211.4 cm^{-1} (9 km/mol), an even worse prediction of the intensity ratio.

To confirm the assignment of the observed bands to the near-linear species, isotopic substitution experiments were performed. Figure 2 shows bands due to the $^{12/13}C$ isotopomers built on the 1827.8 and 1231.6 cm^{-1} bands. The comparison between the observed isotopomer bands and the predicted (scaled) *nl*-$^{107}Ag^{12/13}C_3$ frequencies are listed in Table 2. As found in the study of CuC_3 clusters, the harmonic vibrational frequencies

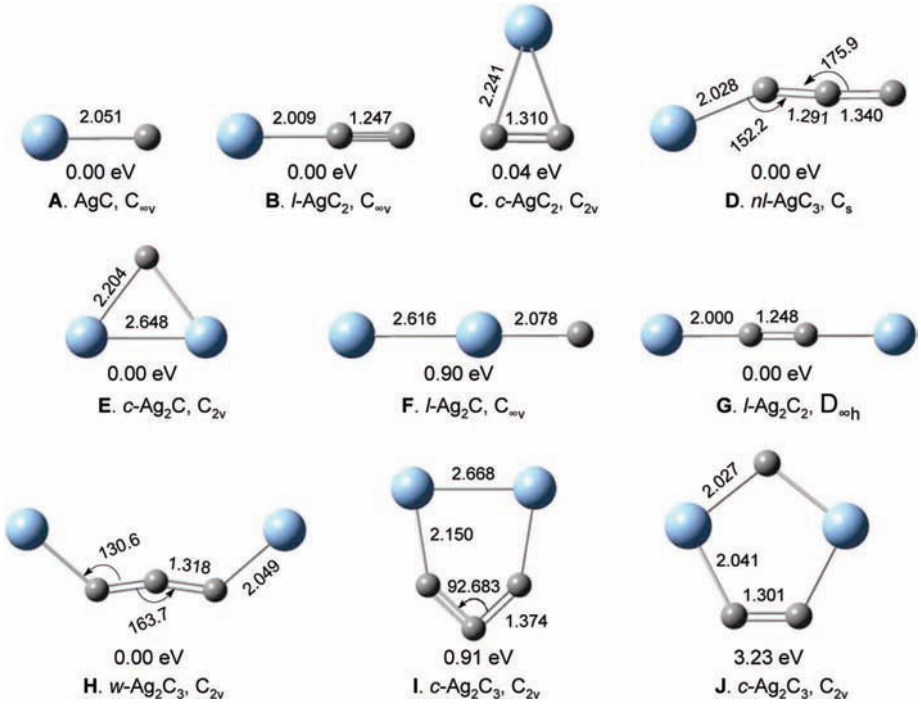

Figure 3. Equilibrium structures for the AgC, AgC_2, AgC_3, Ag_2C, Ag_2C_2, and Ag_2C_3 clusters. The bond lengths (Å) and angles (deg) calculated at the MPW1PW91/SDD level are marked. The relative isomer energies are indicated.

TABLE 2: Comparison of Experimental and Calculated Isotopomer Frequencies (Integral Intensities) for the Asymmetric and Symmetric C═C Stretch Fundamental Modes of Near-Linear $^{107}Ag\ ^{12/13}C_3$

			B3LYP/SDD		MPW1PW91/SDD	
	isotopomer	ν_{exp}[a] (cm^{-1})	ω_{sc}[b] [cm^{-1} (km mol^{-1})]	$\nu_{exp} - \omega_{sc}$ (cm^{-1})	ω_{sc}[c] [cm^{-1} (km mol^{-1})]	$\nu_{exp} - \omega_{sc}$ (cm^{-1})
			Asymmetric C═C Stretch Mode			
a	107−12−12−12	1827.8	1827.8 (133)	0.0	1827.8 (117)	0.0
b	107−12−12−**13**	1823.3	1822.0 (132)	1.3	1823.2 (115)	0.1
c	107−12−**13**−12	1785.5	1782.9 (125)	2.6	1784.1 (108)	1.4
d	107−**13**−12−12	1805.6	1808.1 (132)	−2.5	1805.7 (118)	−0.1
e	107−12−**13**−**13**	1781.5	1777.2 (124)	4.3	1779.7 (106)	1.8
f	107−**13**−12−**13**	1800.5	1801.6 (131)	−1.1	1800.5 (116)	0.0
g	107−**13**−**13**−12	1762.4	1762.3 (125)	0.1	1760.9 (110)	1.5
h	107−**13**−**13**−**13**	1757.6	1755.9 (123)	1.7	1755.8 (108)	1.8
			Symmetric C═C Stretch Mode			
a	107−12−12−12	1231.6	1231.6 (9)	0.0	1231.6 (14)	0.0
b	107−12−12−**13**	1205.8	1205.3 (9)	0.5	1204.8 (15)	1.0
c	107−12−**13**−12	1228.2	1230.0 (9)	−1.8	1229.2 (14)	−1.0
d	107−**13**−12−12	1211.9	1210.4 (8)	1.5	1211.7 (12)	0.2
e	107−12−**13**−**13**	1201.7	1203.2 (9)	−1.5	1201.9 (15)	−0.2
f	107−**13**−12−**13**	1185.3	1184.5 (8)	0.8	1185.3 (12)	0.0
g	107−**13**−**13**−12	1209.7	1209.3 (8)	0.4	1210.0 (12)	−0.3
h	107−**13**−**13**−**13**	1183.9	1183.1 (8)	0.8	1183.2 (13)	0.7

[a] Experimental band energies for symmetric mode are tentative because of their weak intensities. [b] Frequencies are scaled uniformly by scaling factors of 0.9801 for asymmetric mode and 1.0167 for symmetric mode. [c] Frequencies are scaled uniformly by scaling factors of 0.9795 for asymmetric mode and 1.0061 for symmetric mode.

predicted by the MPW1PW91/SDD calculations are in good agreement with the assignment of these bands to *nl*-AgC_3 ($X\ ^2A'$) (structure **D**), whereas the B3LYP/SDD match is again poorer. The maximum differences between experimental and predicted isotopomer frequencies, $\nu_{exp} - \omega_{sc}$, are 4.3 cm^{-1} for B3LYP/SDD and 1.8 cm^{-1} for MPW1PW91/SDD. The average values of these differences for all observed isotopomers (for both modes) are 1.3 cm^{-1} (B3LYP) and 0.63 cm^{-1} (MPW1PW91). Although the 1.8 and 0.63 cm^{-1} values are typical for structures assigned using isotopic ^{13}C labeling, the 4.3 and 1.3 cm^{-1} B3LYP values are too large to be acceptable. Thus, based on the comparison with the MPW1PW91 calculation, we conclude that the *nl*-AgC_3 (structure **D**) was formed in our experiments and is responsible for the two bands at 1827.8 and 1231.6 cm^{-1}.

When silver bonds to either end of the same singly substituted isotopic precursor, i.e., $^{12/13}C_3$ (12−12−**13**), both **b** (107−12−12−**13**) and **d** (107−**13**−12−12) isotopomers can be formed. Figure 3 shows that the **b** and **d** bands have comparable intensities, as expected. Similarly, when Ag attaches to the C_3 (12−**13**−**13**) precursor, both **e** (107−12−**13**−**13**) and **g** (107−**13**−**13**−12) isotopomers are formed. Again, Figure 3 shows that the **e** and **g** bands have similar intensities. In our previous study of CuC_3, we found that the analogous sets of isotopomeric bands were *not* of equal intensity and that this resulted from photoinduced isotopic scrambling of ^{13}C and ^{12}C isotopes in the cluster. The present observation that the bands in the **b**, **d** set and in the **e**, **g** set retain their equal intensities leads to the conclusion that no photoinduced isotopic scrambling takes place in AgC_3. The photoscrambling in CuC_3 and C_3 involves a cyclic intermediate,[27,51,52] but such a stable cyclic structure could not be found for AgC_3.

It is interesting to compare the structural parameters and binding energies of the *nl*-AgC_3 and *nl*-CuC_3 clusters, both calculated at the MPW1PW91/SDD level. The metal−carbon bond lengths (BLs) in *nl*-AgC_3 are much greater than those in *nl*-CuC_3; specifically, BL(Ag—C) = 2.028 Å vs BL(Cu—C) = 1.810 Å. On the other hand, the carbon−carbon BLs are similar. In AgC_3, the C═C BLs are 1.291 and 1.340 Å, whereas in CuC_3, they are 1.287 and 1.342 Å. The Ag—C—C bond angle in *nl*-AgC_3 is significantly smaller (152.2°) than the corresponding bond angle in *nl*-CuC_3 (160.6°). The longer bonds in *nl*-AgC_3 reflect its lower dissociation energy (1.77 eV) compared to 2.38 eV for *nl*-CuC_3. The Ag—C bond is weaker than the Cu—C bond by 0.61 eV, reflecting the larger size of the silver atom.

4.2.4. Ag_2C. The lowest-energy isomers of Ag_2C cluster are triplets of **E** and **F**. Our calculation using MPW1PW91/SDD shows that the **F** (linear) isomer is higher in energy by 0.90 eV. No Ag_2C was observed in our experiments because the highest IR integral intensity for the more stable cyclic isomer **E** is only 4 km/mol and all predicted frequencies are out of the energy range accessible by our FT-IR instrument.

4.2.5. Ag_2C_2. The linear AgC_2Ag cluster (**G**), also known as silver acetylide, is the only stable structure found. This species is predicted to appear at 600.3 cm^{-1} with 78 km/mol integral intensity, but was not observed.

4.2.6. Ag_2C_3. Three stable C_{2v} isomers were found for Ag_2C_3; all are singlets. The w-shaped one (**H**) has the lowest energy, and the other two with cyclic structures, **I** and **J**, are less stable by 0.91 and 3.23 eV, respectively. Table 1 lists the harmonic vibrational frequencies and integral intensities for all three. The most intense mode predicted for **H** is 1761.1 cm^{-1} (639 km/mol), the asymmetric C═C stretch. Although the integral intensities for structures **H**−**J** are all very large, we did not observe any bands assignable to these clusters.

5. Conclusions

New silver−carbon species were sought by simultaneous dual-laser ablation of silver and carbon followed by trapping in solid argon matrixes at 12 K. Two new bands were observed at 1827.8 and 1231.6 cm^{-1}. Based on the results of isotopic ^{13}C-substitution experiments and density functional theory calculations with the MPW1PW91/SDD functional/basis set, these two bands were assigned to the asymmetric and symmetric C═C stretching modes, respectively, in the near-linear AgC_3 cluster.

The calculated dissociation energy at the MPW1PW91/SDD level for *nl*-AgC_3 is 1.77 eV, which is 0.61 eV lower than that

for *nl*-CuC_3. The weaker binding in *nl*-AgC_3 is reflected in its longer metal−carbon bonds compared to those in *nl*-CuC_3.

No photoinduced isotopic scrambling in $^{107}Ag^{12/13}C_3$ isotopomers was observed as was found in $Cu^{12/13}C_3$, a finding consistent with the fact that no stable cyclic structure of doublet AgC_3 could be found theoretically. Such a structure was previously determined to be essential to the photoscrambling found in CuC_3.

The equilibrium structures and vibrational frequencies for AgC, AgC_2, Ag_2C, Ag_2C_2, and Ag_2C_3 were also calculated using MPW1PW91/SDD, but none were observed in our experiments. Although some bands remain unassigned in our spectra, mainly in the 1750−1900 cm^{-1} range, it is likely that they are due to larger clusters of AgC_n ($n > 3$).

Acknowledgment. The authors are grateful to The Petroleum Research Fund, administered by the American Chemical Society, for its support of this research.

References and Notes

(1) Liu, P.; Rodriguez, J. A.; Muckerman, J. T. *J. Phys. Chem. B* **2004**, *108*, 15662.
(2) Liu, P.; Rodriguez, J. A.; Muckerman, J. T. *J. Phys. Chem. B* **2004**, *108*, 18796.
(3) Guo, B. C.; Kerns, K.; Castleman, A. W., Jr. *Science* **1992**, *255*, 1411.
(4) Cartier, S. F.; May, B. D.; Castleman, A. W., Jr. *J. Chem. Phys.* **1994**, *100*, 5384.
(5) Cartier, S. F.; May, B. D.; Castleman, A. W., Jr. *J. Am. Chem. Soc.* **1994**, *116*, 5295.
(6) Leskiw, B. D.; Castleman, A. W., Jr. *C. R. Phys.* **2003**, *3*, 251.
(7) Pilgrim, J. S.; Duncan, M. A. *J. Am. Chem. Soc.* **1993**, *115*, 9724.
(8) Tono, K.; Terasaki, A.; Ohta, T.; Kondow, T. *Chem. Phys. Lett.* **2002**, *351*, 135.
(9) Knappenberger, K. L., Jr.; Jones, C. E., Jr.; Sobhy, M. A.; Iordanov, I.; Sofo, J.; Castleman, A. W., Jr. *J. Phys. Chem. A* **2006**, *108*, 12814.
(10) Knappenberger, K. L., Jr.; Clayborne, P. A.; Reveles, J. U.; Sobhy, M. A.; Jones, C. E., Jr.; Gupta, U. U.; Khanna, S. N.; Iordanov, I.; Sofo, J.; Castleman, A. W., Jr. *ACS Nano* **2007**, *1*, 319.
(11) Wang, L. S.; Li, X. *J. Chem. Phys.* **2000**, *112*, 3602.
(12) Fan, J. W.; Lou, L.; Wang, L. S. *J. Chem. Phys.* **1995**, *102*, 2701.
(13) Zhai, H.; Liu, S. R.; Li, X.; Wang, L. S. *J. Chem. Phys.* **2001**, *115*, 5170.
(14) Wang, X. B.; Ding, C. F.; Wang, L. S. *J. Phys. Chem. A* **1997**, *101*, 7699.
(15) Kohno, M.; Suzuki, S.; Siromaru, H.; Kobayashi, K.; Nagase, S.; Achiba, Y.; Kietzmann, H.; Kessler, B.; Gantefor, G.; Eberhardt, W. *J. Electron Spectrosc.* **2000**, *112*, 163.
(16) Yamada, Y.; Castleman, A. W., Jr. *Chem. Phys. Lett.* **1993**, *133*, 204.
(17) Datta, B. P.; Raman, V. L.; Subbanna, C. S.; Jain, H. C. *Int. J. Mass Spectrom. Ion Process.* **1989**, *91*, 241.
(18) Robbins, D. L.; Rittby, C. M. L.; Graham, W. R. M. *J. Chem. Phys.* **2001**, *114*, 3570.
(19) Kinzer, R. E., Jr.; Rittby, C. M L.; Graham, W. R. M. *J. Chem. Phys.* **2006**, *125*, 074513.
(20) Bates, S. A.; Rittby, C. M. L.; Graham, W. R. M. *J. Chem. Phys.* **2006**, *125*, 074506.
(21) Bates, S. A.; Rhodes, J. A.; Rittby, C. M. L.; Graham, W. R. M. *J. Chem. Phys.* **2007**, *127*, 064506.
(22) Bates, S. A.; Rittby, C. M. L.; Graham, W. R. M. *J. Chem. Phys.* **2008**, *128*, 234301.
(23) Kinzer, R. E.; Rittby, C. M. L.; Graham, W. R. M. *J. Chem. Phys.* **2008**, *128*, 064312.
(24) Cataldo, F. *J. Raman Spectrosc.* **2008**, *39*, 169.
(25) Sakurai, H.; Castleman, A. W., Jr. *J. Phys. Chem. A* **1998**, *102*, 10486.
(26) Wang, L. S.; Li, S.; Wu, H. *J. Phys. Chem.* **1996**, *100*, 19211.
(27) Szczepanski, J.; Wang, Y.; Vala, M. *J. Phys. Chem. A* **2008**, *112*, 4778.
(28) Vogel, A. I. *Practical Organic Chemistry*, 3rd ed.; Longmans: London, 1967.
(29) Bahr, G.; Burba, P. In *Methoden der Organischen Chemie*; Houben-Weyl Thieme-Verlag: Stuttgart, Germany, 1970; Vol. 13, Part I, pp 767.
(30) Frisch, M. J.; Trucks, G. W.; Schlegel, H. B.; Scuseria, G. E.; Robb, M. A.; Cheeseman, J. R.; Montgomery, J. A., Jr.; Vreven, T.; Kudin, K. N.; Burant, J. C.; Millam, J. M.; Iyengar, S. S.; Tomasi, J.; Barone, V.; Mennucci, B.; Cossi, M.; Scalmani, G.; Rega, N.; Petersson, G. A.; Nakatsuji, H.; Hada, M.; Ehara, M.; Toyota, K.; Fukuda, R.; Hasegawa, J.; Ishida, M.; Nakajima, T.; Honda, Y.; Kitao, O.; Nakai, H.; Klene, M.; Li, X.; Knox, J. E.; Hratchian, H. P.; Cross, J. B.; Bakken, V.; Adamo, C.; Jaramillo, J.; Gomperts, R.; Stratmann, R. E.; Yazyev, O.; Austin, A. J.; Cammi, R.; Pomelli, C.; Ochterski, J. W.; Ayala, P. Y.; Morokuma, K.; Voth, G. A.; Salvador, P.; Dannenberg, J. J.; Zakrzewski, V. G.; Dapprich, S.; Daniels, A. D.; Strain, M. C.; Farkas, O.; Malick, D. K.; Rabuck, A. D.; Raghavachari, K.; Foresman, J. B.; Ortiz, J. V.; Cui, Q.; Baboul, A. G.; Clifford, S.; Cioslowski, J.; Stefanov, B. B.; Liu, G.; Liashenko, A.; Piskorz, P.; Komaromi, I.; Martin, R. L.; Fox, D. J.; Keith, T.; Al-Laham, M. A.; Peng, C. Y.; Nanayakkara, A.; Challacombe, M.; Gill, P. M. W.; Johnson, B.; Chen, W.; Wong, M. W.; Gonzalez, C.; Pople, J. A. *Gaussian 03*, revision B.05; Gaussian, Inc.: Pittsburgh, PA, 2004.
(31) Perdew, J. P.; Wang, Y. *Phys. Rev. B* **1992**, *45*, 132444.
(32) Adamo, C.; Barone, V. *J. Chem. Phys.* **1998**, *102*, 1995.
(33) Andrae, D.; Haeussermann, U.; Dolg, M.; Stoll, M.; Preuss, H. *Theor. Chim. Acta* **1990**, *77*, 123.
(34) Chan, W.-T.; Fournier, R. *Chem. Phys. Lett.* **1999**, *315*, 257.
(35) Hamilton, I. P. *Chem. Phys. Lett.* **2004**, *390*, 517.
(36) Wiberg, K. *J. Comput. Chem.* **1999**, *20*, 1299.
(37) Dunbar, R. *J. Phys. Chem.* **2002**, *106*, 7328.
(38) Oomens, J.; Moore, D. T.; von Helden, G.; Mejier, G.; Dunbar, R. *J. Am. Chem. Soc.* **2004**, *126*, 724.
(39) Szczepanski, J.; Wang, H.; Vala, M.; Tielens, A. G. G. M.; Eyler, J. R.; Oomens, J. *Astrophys. J.* **2006**, *646*, 666.
(40) Wang, Y.; Szczepanski, J.; Vala, M. *Chem. Phys.* **2007**, *342*, 107.
(41) Becke, A. D. *J. Chem. Phys.* **1993**, *98*, 5648.
(42) Weltner, W., Jr.; Van Zee, R. J. *Chem. Rev* **1989**, *89*, 1713.
(43) Van Orden, A.; Saykally, R. J. *Chem. Rev.* **1998**, *98*, 2313.
(44) Szczepanski, J.; Auerbach, E.; Vala, M. *J. Phys. Chem.* **1997**, *101*, 9296.
(45) Jacox, M. E.; Milligan, D. E. *Chem. Phys.* **1974**, *4*, 45.
(46) Jiang, Q.; Rittby, C. M. L.; Graham, W. R. M. *J. Chem. Phys.* **1993**, *99*, 3194.
(47) Andrews, L.; Kushto, G. P.; Zhou, M.; Wilson, S. P.; Souter, P. F. *J. Chem. Phys.* **1999**, *110*, 4457.
(48) Ding, X. D.; Wang, S. L.; Rittby, C. M. L.; Graham, W. R. M. *J. Chem. Phys.* **2000**, *112*, 5113.
(49) Kranze, R. H.; Graham, W. R. M. *J. Chem. Phys.* **1993**, *98*, 71.
(50) Szczepanski, J.; Ekern, S.; Vala, M. *J. Phys. Chem.* **1995**, *99*, 8002.
(51) Szczepanski, J.; Vala, M. *Eur. Phys. J.: Special Top.* **2007**, *144*, 27.
(52) Fueno, H.; Taniguchi, Y. *Chem. Phys. Lett.* **1999**, *312*, 65.

JP805181M